HD-EQNN: High-dimensional Ensemble Quantum Neural Network for Multi-class UAV Signal Recognition

Wenxia Wang[1], Hanyun Wang[2], Xin Zhou[1], Yaqi Chen[3], Yifan Hou[1], Jinchen Xu[1*]
[1]School of Cyberspace Security, Information Engineering University, Zhengzhou, China
[2]School of Electronics and Communication Engineering, Sun Yat-sen University, Shenzhen, China
[3]School of Information System Engineering, Information Engineering University, Zhengzhou, China
yingluobinfen@sina.cn, wanghanyun@mail.sysu.edu.cn, qf_zhouxin@126.com,
chyaqi163@163.com, hou3938268@126.com, atao728208@126.com

***Abstract*—Under the constraints of current quantum hardware, there are challenges in using quantum neural networks (QNNs) to perform multi-classification for high-dimensional signal features. In this paper, a high-dimensional ensemble quantum neural network (HD-EQNN) is proposed for multi-classification of frequency-domain signals, achieving an end-to-end mapping from Doppler spectrum to recognition results. The core components of HD-EQNN are the feature extraction module, the feature fusion module, and the ensemble learning classification module. The feature extraction module is capable of simultaneously rotational encoding 128-dimensional features into the same model, capturing local dependencies in groups. The feature fusion module fuses independent intermediate features to maintain the integrity of frequency domain information. The ensemble learning classification module uses multiple QNNs to form a strong learner to effectively capture global complex relationships. The modules cooperate with each other to automatically extract features and realize multi-classification. Experiments on two real UAV radar echo signal datasets show that in multi-class UAV signal recognition tasks, the accuracy of HD-EQNN is superior to existing quantum models, and it uses fewer quantum resources than amplitude encoding quantum methods. This advancement provides an effective solution for applying quantum methods to handle complex signals in the real world during the NISQ era.**

Keywords—quantum neural network, end-to-end, high-dimensional features, ensemble learning, unmanned aerial vehicle

I. INTRODUCTION

Quantum neural networks (QNNs) represent an emerging research field that combines quantum computing with neural networks. It is also a popular direction that is continuously explored in the current field of quantum computing [1]-[4]. Existing studies have shown that QNN has the potential advantage of a larger effective dimension and can achieve good generalization ability from a small number of training samples [5]-[7]. The theoretical research on QNNs has gradually matured, but there has been relatively little exploration in complex multi-classification problems in the real world. With the advantages of flexible mobility, low cost, and convenient operation, Unmanned Aerial Vehicles (UAVs) are widely used in precision agriculture [8], [9], auxiliary communication [10], [11], infrastructure supervision [12], traffic detection [13], and other fields. However, there are also potential safety risks, such as privacy protection issues and threats to aviation security. The use of radar systems to quickly, accurately, and remotely identify UAVs is one of the current research hotspots in the field of low-altitude security protection [14],[15]. Combining QNN to directly identify the types of UAVs from real radar echo signals has significant practical value, but there are also many difficulties.

In the NISQ era, the number of qubits and the depth of quantum circuits are limited [16], and there are significant challenges in using QNN to automatically extract high-dimensional features. The common encoding methods include amplitude encoding and rotational encoding. Amplitude encoding comes with a high cost of quantum encoding. For example, the Doppler spectrum used for UAV identification contains 128-dimensional features. Amplitude encoding, when encoding these features, introduces 247 quantum gates and a 241-layer circuit depth to the quantum circuit. The anti-decoherence capability of large-scale quantum circuits is weak, making it difficult to execute stably on a real quantum machine [17], [18]. The use of rotational encoding also poses problems. One of them is that large-scale quantum circuits exceed the simulation capabilities of classical simulators. Secondly, the decoherence effect of real quantum machines can affect the execution performance of large-scale quantum circuits. One approach is to first perform dimensionality reduction using the PCA method and then rotationally encode the data. However, the classical dimensionality reduction process leads to information loss, and the obtained information may not be suitable for quantum methods. Therefore, it is necessary to study a method that uses small-scale quantum resources to automatically extract high-dimensional features.

In the Doppler spectrum, the features that can effectively identify the UAV are distributed within several consecutive local frequency domain sections. When designing the feature extraction module of the high-dimensional ensemble quantum neural network (HD-EQNN), it was considered to use multiple small QNNs instead of directly inputting all high-dimensional features into a large QNN. Multiple small QNNS work together to achieve the grouped automatic extraction of high-dimensional frequency-domain features. The independent features extracted in groups can only reflect the dependency relationships within local frequency domain segments. Therefore, a feature fusion module is introduced to ensure the integrity of the frequency domain information.

Furthermore, designing high-performance and highly stable multi-class quantum methods is one of the key research focuses and challenges in quantum machine learning in the NISQ era [19]-[21]. We apply the ensemble learning strategy [22],[23], treating QNN as a base learner. Multiple base learners are jointly trained to form a strong learner, which jointly makes decisions on the type of UAV. Each base learner focuses on different features. During the joint training process, the parameters of each base learner are dynamically adjusted,

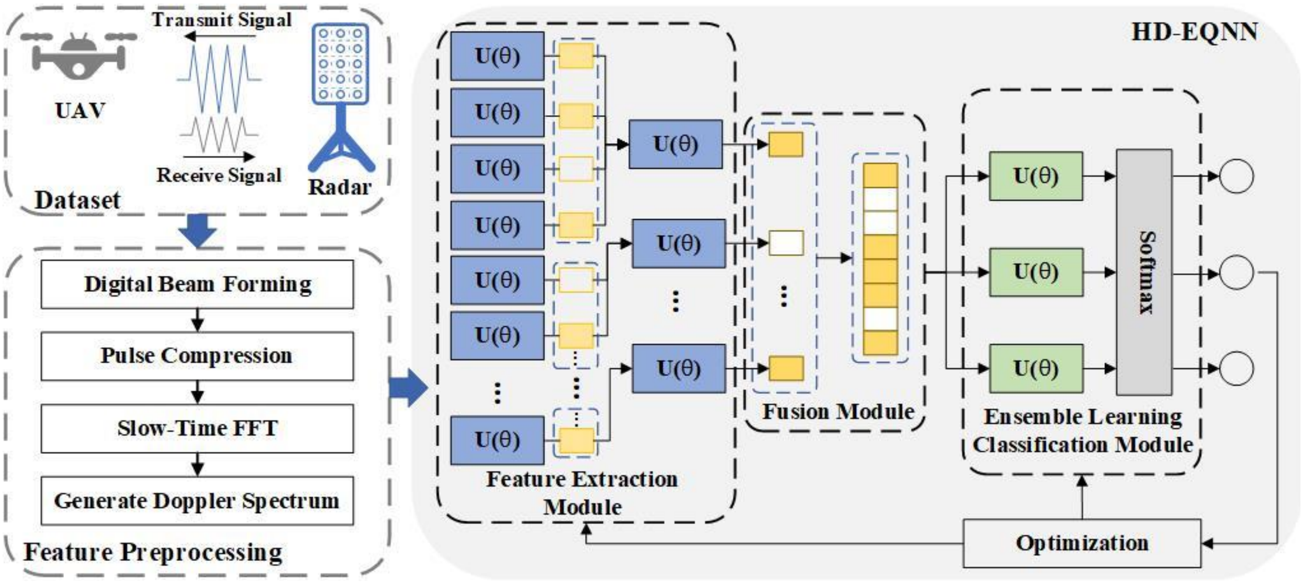

Fig. 1. Flowchart. The identification process of the real UAV radar echo signal dataset includes feature preprocessing and HD-EQNN. The feature extraction module and the ensemble learning classification module of HD-EQNN are both composed of several small QNNs.

which can improve the performance of multi-classification and enhance the stability of the model. The high-dimensional Doppler spectrum feature has undergone a processing procedure of local compression, global fusion, and integrated amplification, which finally leads to the decision result.

The contributions of this article are as follows:

- A novel joint-optimization QNN architecture is proposed, which automatically completes feature extraction and classification decision-making in a quantum model. This architecture takes the 128-dimensional Doppler spectrum as the input and directly outputs the UAV category. End-to-end optimization is achieved through joint training.
- A frequency-domain feature processing method suitable for QNN is proposed. This method first groups the high-dimensional features and then integrates them. Multiple small QNNs capture the dependencies within high-frequency or low-frequency sections to reduce the quantum resource requirements. Integrate the independent features extracted by each QNN to maintain the integrity of the frequency domain information. This enables the QNN to automatically extract high-dimensional features with low resources.
- Propose a QNN ensemble learning method for multi-class UAV signal recognition. This method uses multiple QNNs of the same structure as the base learners. Softmax is introduced for probability normalization to effectively integrate the discriminative confidence of each base learner.
- Experimental results show that, compared with other quantum models, HD-EQNN achieves the highest accuracy on two real UAV radar echo datasets. Compared with the quantum method using amplitude encoding, the quantum circuit scale of HD-EQNN is only one-third of that.

Due to security restrictions, the code is available from the corresponding author, subject to institutional approval.

II. METHODOLOGY

A. Overall Process

The workflow includes classic feature preprocessing and HD-EQNN (Fig. 1). The classic feature preprocessing transforms the dataset into a Doppler spectrum. HD-EQNN automatically groups Doppler spectrum features, captures their dependencies, and identifies the type of UAV. The entire process is expressed as:

$$acc = \frac{1}{n}\sum_{i=1}^{n} \mathbb{I}(label_i = HDEQNN_\theta(Pre(S_i))) \quad (1)$$

where n represents the total number of signal samples. S_i denotes the radar echo signal of the UAV. Pre(·) indicates feature preprocessing. $HDEQNN_\theta(\cdot)$ represents the predicted category of the UAV. $\mathbb{I}(\cdot)$ takes the value of 1 when the condition is met, and 0 otherwise. $label_i$ is the true classification label of the i-th sample.

The classic feature preprocessing stage performs feature preprocessing on the UAV radar echo signals collected by the radar equipment. Through signal processing operations such as Digital Beam Forming (DBF), Pulse Compression (PC), Slow-Time FFT Processing, and Generate Doppler Spectrum (GDS), the signals from the antenna array are converted into Doppler spectra that can identify the UAV.

HD-EQNN consists of a feature extraction module, a feature fusion module, an ensemble learning classification module, and a classical unified optimization module. The feature extraction module and the ensemble learning classification module are both composed of several small QNNs. These small QNNs are similar to the existing QNNs, including the quantum encoding layer, parameterized quantum circuit layer, and measurement layer, but they do not have an optimization module. The feature fusion module integrates the independent local features extracted by each QNN. The unified optimization module synchronously adjusts the parameters of the QNNs in the feature extraction module and the ensemble learning classification module through backpropagation, achieving the collaborative update of

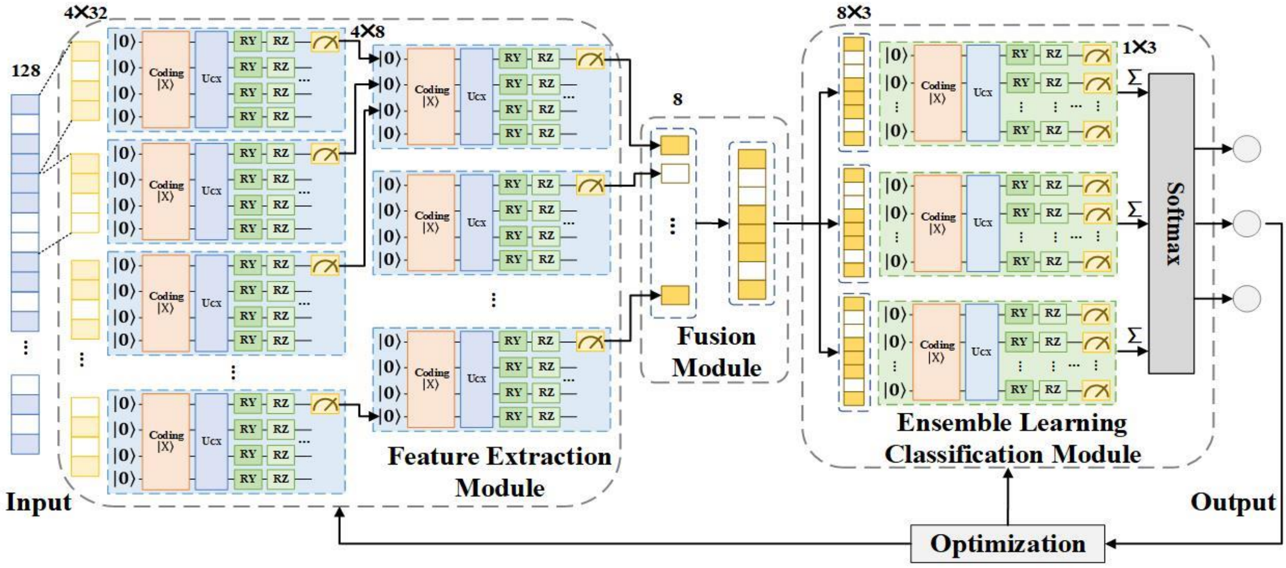

Fig. 2. HD-EQNN structure diagram.

feature learning and classification decisions. Next, we will provide a detailed introduction to each of the steps.

B. Feature Preprocessing

Feature preprocessing analyzes the signal characteristics of UAV radar echo signals and extracts the Doppler spectrum. DBF moves signal processing to the digital domain. In the digital domain, beamforming performs a weighted summation on the eight channels of the received signal. Expressed as:

$$B(j) = \sum_{i=1}^{8} D(i,j) \;\; j = 1,2,\dots,128 \tag{2}$$

where *i* represents the index of the receiving channel, and *j* represents the index of the pulse echo.

Pulse Compression can simultaneously ensure the effective range and the range resolution of the radar system. Use linear frequency modulation signals (LFM) to encode wide pulses. The transmission reference signal LFM is expressed as:

$$s(t) = \mathrm{rect}(\tfrac{t}{T}) e^{j\pi K t^2} \tag{3}$$

where *t* represents the time variable. *T* is the duration of the signal pulse. $K = \frac{\mathrm{B}}{\tau}$, where **B** represents the signal bandwidth, and τ represents the signal pulse width. At the receiving end, the PC uses matched filtering to compress the echo signal into a narrow pulse, thereby achieving high-resolution detection. Matched filtering is:

$$Y(k) = R(k) \cdot \overline{S(k)} \tag{4}$$

where $R(k) = \sum_{n=0}^{N-1} r(n) e^{-j\frac{2\pi}{N}kn}, k = 0,1,\dots,N-1$ is the Fourier transform of the received signal. $S(k) = \sum_{n=0}^{N-1} s(n) e^{-j\frac{2\pi}{N}kn}, k = 0,1,\dots,N-1$ is the Fourier transform of the transmitted reference signal.

The Slow-Time FFT, in combination with the Doppler formula, performs an FFT on each fixed distance unit after PC. This process separates targets of different speeds and forms a range-doppler image. The Doppler formula is [24]:

$$f_d = \frac{2v}{\lambda} \tag{5}$$

where f_d represents the Doppler frequency, and λ is the wavelength of the transmitted signal. v represents the radial velocity of the target relative to the radar (m/s).

Finally, based on the specific distance unit where the UAV is located, a Doppler spectrum of the UAV will be generated. In the Doppler spectrum, the distribution of micro-Doppler lines generated by the rotors of different types of UAVs is obviously different, which is the key feature for identifying these UAVs.

Feature preprocessing converts the radar echo signals into a form that can determine the type of UAV, preventing them from being overwhelmed by ground clutter and other interferences. There are significant differences among the Doppler spectra of various types of UAVs. There are subtle differences in the Doppler spectra of UAVs within the same category. Therefore, the 128-dimensional Doppler spectrum data were input into the HD-EQNN, and features were automatically extracted to identify different types of UAVs.

C. High-dimensional Ensemble Quantum Neural Network

The HD-EQNN takes in a 128-dimensional Doppler spectrum as input, capturing the inherent correlations and enabling multi-class identification of UAVs. HD-EQNN consists of a feature extraction module, a feature fusion module, an ensemble learning classification module, and a classical unified optimization module.

1) Small QNN: The feature extraction module and the ensemble learning classification module are both composed of multiple small QNNs. The small QNN consists of an encoding layer, a parameterized quantum circuit, and a measurement layer. The difference from common QNNs is that the small QNN in HD-EQNN does not have an optimization module. The encoding layer uses rotational encoding. The parameterized quantum circuit is a stack of multiple Ansatz. The Ansatz provides a parameterized unitary transformation $U(\theta)$. By adjusting the parameter θ, different quantum states can be represented. The measurement layer measures the quantum state multiple times to obtain the circuit result. The small QNN of the feature extraction module measures the probability of a single qubit as a result. The small QNN of the ensemble learning classification module measures the state of the quantum circuit and stores it in vector form. The post-processing yields one-dimensional data as the result. The small QNN is represented as:

$$QNN(x,\theta) = |U_l(\theta_l)U_{l-1}(\theta_{l-1}) \dots U_0(\theta_0)\rangle |e(x)\rangle |\varphi_{ini}\rangle \quad (6)$$

where $|\varphi_{ini}\rangle$ represents the randomly initialized value. $|e(x)\rangle$ represents the encoding process. $|U_l(\theta_l)U_{l-1}(\theta_{l-1}) \dots U_0(\theta_0)\rangle$ represents the parameterized quantum circuit of the Ansatz stack. And l represents the number of stacking layers.

2) Feature extraction module: The feature extraction module realizes the automatic extraction of high-dimensional frequency-domain features. This module utilizes multiple small quantum circuits to perform the functions of a large quantum circuit, thereby enhancing the decoherence resistance capability of the quantum circuit. Multiple small QNNs collaboratively process high-dimensional features grouped by frequency domain segments.

The design concept of the feature extraction module is derived from the local frequency domain segment idea. The micro-Doppler characteristics differences of UAVs are mainly manifested in several different frequency domain sections. Each small QNN extracts the features of different local frequency domain segments and captures the local dependencies. The larger the frequency domain segment is, the greater the frequency domain range for the small QNN processing becomes, and it also means that more global features are contained. The smaller the frequency domain section is, the more local and detailed the features tend to be.

Specifically, the high-dimensional feature vector $V = [v_1, v_2, \dots, v_n]$ obtained through feature preprocessing is grouped by the feature extraction module according to frequency domain segments. After grouping, we obtain g feature groups $vg_i = [v_1, v_2, \dots, v_j], i \in (1, g)$, where j represents the number of features contained in the frequency domain segment. In this way, the feature frequency domains within the same group are similar, reducing the mutual interference between high-frequency and low-frequency features during feature extraction. The grouped features are input to the feature extraction module for extracting high-level features.

The feature extraction module consists of several feature extraction layers FEL_x. Each feature extraction layer consists of several parallel small $QNN_{x,y}$. The number of $QNN_{1,y}$ in the first feature extraction layer is the same as the number of frequency domain segments. The number of qubits in these $QNN_{1,y}$ is the same as the number of features within the frequency domain segment. Each group of shallow features vg_i is rotationally encoded into $QNN_{1,i}$. After the execution of the circuit, $QNN_{1,i}$ obtains the independent middle-level feature $fev_{1,i}$. The feature fusion module concatenates the independent middle-level features extracted by each small QNN to obtain the fused middle-level feature $fev\_mid_1 = [fev_{1,1}, fev_{1,2}, \dots fev_{1,g}]$. The second feature extraction layer further groups and extracts features from the intermediate feature fev_mid_1. The construction and processing of the higher-level feature extraction layer is similar. The number of layers in the feature extraction layer and the number of small QNNs contained in each layer can be dynamically expanded and can be adjusted and optimized according to the characteristics of the feature vector. The above process can be expressed as:

$$FEM(\theta) = \prod_{x=1}^{l} FEL_x(\theta_x) = \prod_{x=1}^{l} \otimes_{y=1}^{m} QNN_{x,y}(\theta_{x,y}) \quad (7)$$

where l represents the number of layers in the feature extraction layer. m represents the number of parallel small QNNs in this layer. $\theta_{x,y}$ represents the parameters contained in a small QNN. The number of parameters contained in $\theta_{x,y}$ is denoted as $p(\theta_{x,y})$. The total number of parameters contained in the entire feature extraction layer is:

$$P_{FEM}(\theta) = \sum_{x=1}^{l} \sum_{y=1}^{m} p(\theta_{x,y}) \quad (8)$$

3) Feature fusion module: The features extracted by each small QNN are independent of each other, and the independent features can only reflect the local dependency relationships. The feature fusion module combines various independent features to obtain a complete high-level feature. In this way, the higher level can acquire global information, thereby maintaining the integrity of the frequency domain information. The feature fusion module is not only used between the feature extraction module and the ensemble learning classification module, but also within the feature extraction module.

4) Ensemble learning classification module: The ensemble learning classification module performs multi-classification on the complete high-level features, capturing global dependencies to identify different types of UAVs. This module combines and normalizes the prediction results of multiple base learners to form a strong learner. Compared to a single learner, a strong learner has better performance and stability.

The base learners of the ensemble learning classification module are small QNNs of the same structure. The number of qubits in each QNN is the same as the dimension of the complete high-level feature. The number of base learners is the same as the number of UAV types. Each base learner represents a type of UAV. The complete high-level features are simultaneously rotationally encoded into each base learner. These parallel base learners are represented as:

$$ELM(\theta) = \otimes_{i=1}^{c} QNN_i(\theta_i) \quad (9)$$

where c represents the number of UAV categories.

The base learner obtains the confidence level z_k for this type of UAV through a series of controlled physical evolutions. These confidence levels are combined into a vector $\mathbf{z} = [z_1, z_2, \dots, z_c]$, where n represents the type of the UAV. The confidence vector is transformed into a probability distribution through the Softmax function. Through joint training, HD-EQNN automatically learns how to optimally utilize the prediction results of multiple base learners. If the output of a certain QNN for a correct category is higher, then it will have a higher probability after the Softmax operation. Each parameterized quantum circuit of the base classifier contains $p(\theta_i)$ parameters. The total number of parameters included in the ensemble learning classification module is:

$$P_{ELM}(\theta)=\sum_{i=1}^{c} p(\theta_i) \quad (10)$$

The total number of parameters of HD-EQNN is:

$$P(\theta)=P_{FEM}(\theta)+P_{ELM}(\theta) \quad (11)$$

5) Classic unified optimization module: Among many other methods, QNN has its own classical optimization modules. In HD-EQNN, the small QNNS in the feature extraction module and the ensemble learning classification module do not have separate classic optimization modules. The HD-EQNN updates the parameters of all quantum circuits using a classic unified optimization module to minimize the loss function. The loss function is expressed as:

$$Loss(label, pre) = -\sum_{i=1}^{n} label_i log(pre_i) \quad (12)$$

Overall, the high-dimensional Doppler spectral features in the HD-EQNN undergo a processing procedure of local compression, global fusion, and integrated amplification. The feature extraction module groups the high-dimensional features and then performs information distillation to extract the independent core features that are strongly relevant to the task. The feature fusion module combines the independent high-level features. The ensemble learning classification module uses multiple base learners to collaboratively learn high-level fusion features, capture global dependencies, and obtain the final decision. The classic unified optimization module jointly optimizes all the parameters. Each module collaborates with the others, achieving an efficient transformation from feature extraction to collaborative decision-making.

III. Experiment

A. Experimental Scenario

The experimental data are from the Ground-Based Radar Detection Dataset of “Low Slow Small” Unmanned Aerial Vehicles Under Simple Field Background Conditions [25]. There are two experimental datasets. When the pulse repetition period is 1000 μs, it is Dataset 1. The target models are DJI M300 and M30T multi-rotor UAVs, as well as JOUAV CW-10 lightweight compound-wing UAVs. The sample size of Dataset 1 is 139. When the pulse repetition period is 533.3 μs, it is Dataset 2. The target models are DJI Inspire 2, Mavic Air 2, and M300 multi-rotor UAVs. The sample size of Dataset 2 is 264.

In the experiment, a neural network framework was built using TensorFlow, and TensorCircuit was employed to simulate the quantum circuits. During the training process, the batch_size was set to 128, and the number of epochs was set to 300. The loss function uses Categorical Crossentropy. The model parameters were iteratively optimized using the Adam optimization algorithm with a learning rate of 0.02.

B. Results and Discussion

1) Performance comparison: Compare the performance of HD-EQNN with that of the classical multi-classification algorithm and the quantum multi-classification algorithm. The classic multi-classification algorithms are BernoulliNB [26] and Bagging [27]. The quantum multi-classification algorithms are HQNNS [28] and SPQCC [29]. To facilitate the experimental analysis, the small QNN of HD-EQNN uniformly adopts a fixed Ansatz structure for stacking in the experiments. Stacked 3 layers of Ansatz. The result is shown in Fig. 3.

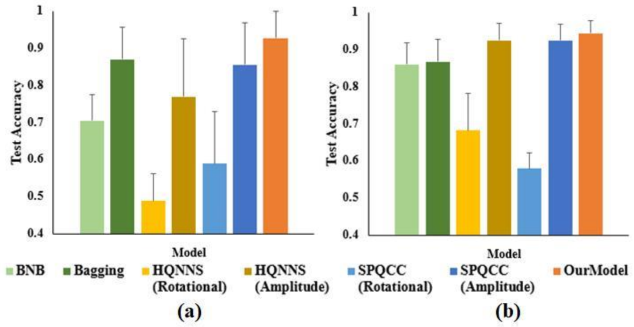

Fig. 3. The mean and standard deviation of the test accuracy of multi-classification experiments. (a) shows the three-classification results of Dataset 1. (b) shows the three-classification results of Dataset 2. The accuracy of HD-EQNN is the highest.

On Dataset 1, HD-EQNN’s average accuracy is 0.9278, and the accuracy standard deviation is 0.0719. On Dataset 2, HD-EQNN’s average accuracy is 0.9434, and the accuracy standard deviation is 0.0353. Compared with other algorithms, HD-EQNN demonstrates a more significant performance advantage in the UAV recognition task. Rotational encoding HQNNS and SPQCC using rotational encoding relies on PCA for dimensionality reduction of features, which cannot fully represent the complex features of UAV radar echo signals, and has the lowest recognition accuracy. Although HQNNS and SPQCC amplitude encoded can automatically extract features, they lack focused attention to key features and have limited recognition performance. The high recognition ability of HD-EQNN stems from its ability to automatically extract features and conduct multi-classification through ensemble learning. The quantum circuit grouping captures the local dependence of high-dimensional frequency domain features and combines

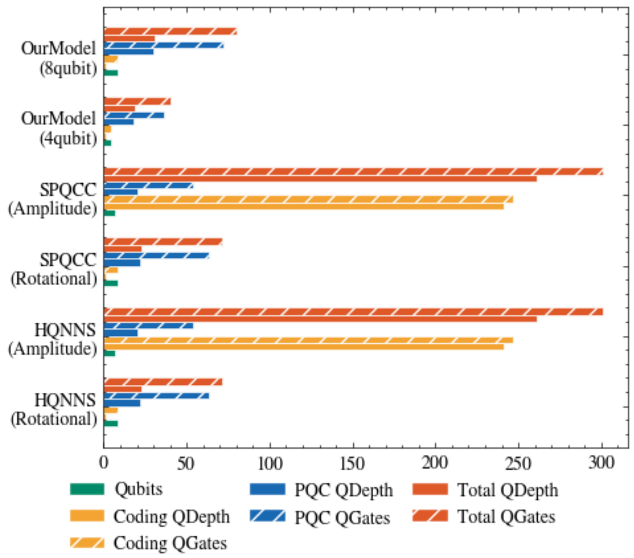

Fig. 4. Comparison of resources for different quantum algorithms. The resource usage of the QNN for each model, including the number of qubits (Qubits), the depth of the quantum circuit (QDepth), and the number of quantum operation gates (QGates). The quantum circuit scale of HD-EQNN is smaller than that of the quantum algorithm using Amplitude encoding.

the global dependence to perform multi-classification, realizing the closed loop of quantum computing from feature self-extraction to multi-classification. This design makes the extracted features more in line with the essential characteristics of quantum computing. The ensemble learning strategy further enhances the model's recognition ability, ultimately achieving an effective improvement in the accuracy of HD-EQNN.

2) Resource comparison: This section analyzes the resource usage of HD-EQNN and other quantum machine learning algorithms. The quantum circuit size of a single QNN is counted. The feature extraction module of HD-EQNN uses 4-qubit quantum circuits, and the ensemble learning classification module uses 8-qubit quantum circuits. When running quantum programs on a real quantum computer, the size of the quantum circuits during the encoding stage also affects the anti-decoherence capability of the overall circuits [30]. Therefore, when making the comparison, the quantum resources used in the encoding part were also taken into account. The result is shown in Fig. 4.

As shown in Fig. 4, the depth of the quantum circuit and the number of quantum gates of HD-EQNN are both much smaller than those of HQNNS and SPQCC that use amplitude encoding. Although the parameterized quantum circuits of HQNNS and SPQCC using amplitude encoding have relatively smaller scales, the quantum circuit depth of the encoding part is 241, and the number of quantum gates is 247.This results in the total quantum circuit depth being 8.42 times that of the 8-qubit HD-EQNN and 13.74 times that of the 4-qubit HD-EQNN. The number of total quantum gates is 3.76 times that of the 8-qubit HD-EQNN and 7.53 times that of the 4-qubit HD-EQNN. Theoretically, the HD-EQNN that uses fewer resources has a stronger anti-decoherence capability.

The amount of resources used by 4-qubit HD-EQNN is less than that of HQNNS and SPQCC using rotational encoding. The amount of resources used by 8-qubit HD-EQNN is slightly higher than that of the HQNNs and SPQCCs that use rotational encoding. However, the recognition accuracy of HQNNS and SPQCC using rotational encoding is relatively low, and it fails to meet the requirements of practical tasks.

The HD-EQNN not only ensures high recognition accuracy but also uses fewer resources compared to the quantum algorithm using amplitude encoding. This advantage stems from the concept of using multiple small QNNs to form a feature extraction module. Replacing a large QNN with multiple small ones enables the extraction of high-dimensional features in groups, and each small QNN uses fewer resources.

3) The performance advantages of ensemble learning: In this experiment, the performance advantages brought about by using ensemble learning methods are discussed. Replace the three QNNs in the ensemble learning module of the model with a single QNN of the same structure. Use the output of only one QNN for three-class classification.

As can be seen from Fig. 5, in both Dataset 1 and Dataset 2, the HD-EQNN with the integrated learning module has a higher average accuracy and a lower standard deviation of accuracy. This indicates that the use of the integrated learning module can effectively improve the accuracy of multi-class classification and also has better stability. This advantage stems from the concept of integrating multiple base learners.

The ensemble learning module effectively improves the performance of HD-EQNN and enhances the stability of HD-EQNN. This is because each QNN in the ensemble learning module has a different initialization state, which can generate different feature representations during the learning process, increase diversity, and thereby enhance the overall performance of the model. Each QNN focuses on different features, thereby enhancing the stability of the model when combined.

4) The impact of different structures on performance:

a) Stacking different layers of Ansatz: In this experiment, the influence of stacking different numbers of Ansatz layers into a QNN on the learning effect of HD-EQNN was analyzed. The result is shown in Fig. 6.

As the number of Ansatz layers in the QNN increases from 1 to 3, the learning performance of the model gradually improves. When the number of Ansatz layers is 1 or 2, the quantum circuits are relatively shallow, the model capacity is insufficient, and it cannot fully fit the effective features in the data, resulting in poor performance. When the number of Ansatz layers is 3, the model structure has the strongest match with the data features and can accurately capture the data patterns. Therefore, it achieves the best learning effect. When the number of Ansatz layers continued to increase to 4, there was no significant improvement in the model performance.

The performance of the model in the multi-classification task of identifying radar echo signals from UAVs is affected

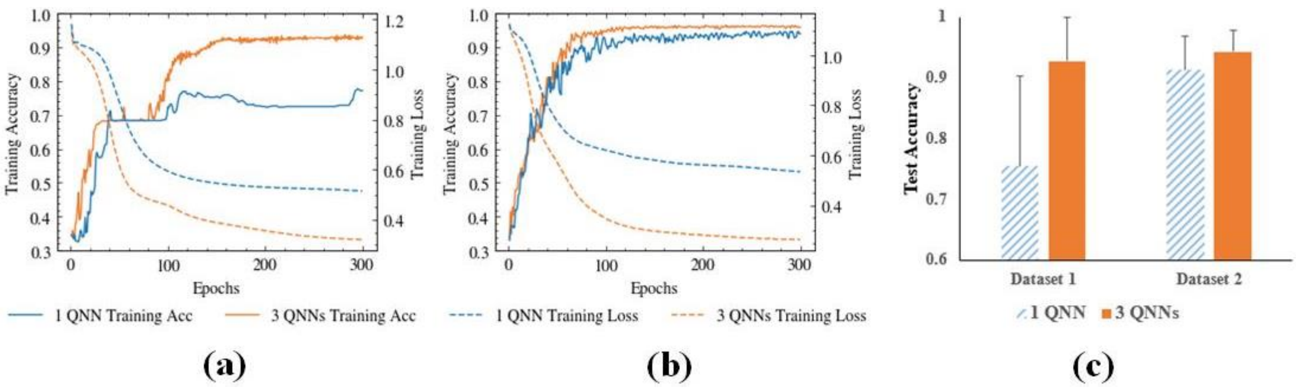

Fig. 5. The performance difference between using ensemble learning and not using ensemble learning. 3QNNs represent the results obtained through ensemble learning. 1QNN represents the results without using ensemble learning. (a) Training curve for Dataset 1. (b) Training curve for Dataset 2. (c) The test accuracy for the two datasets. Using ensemble learning has higher accuracy and greater stability.

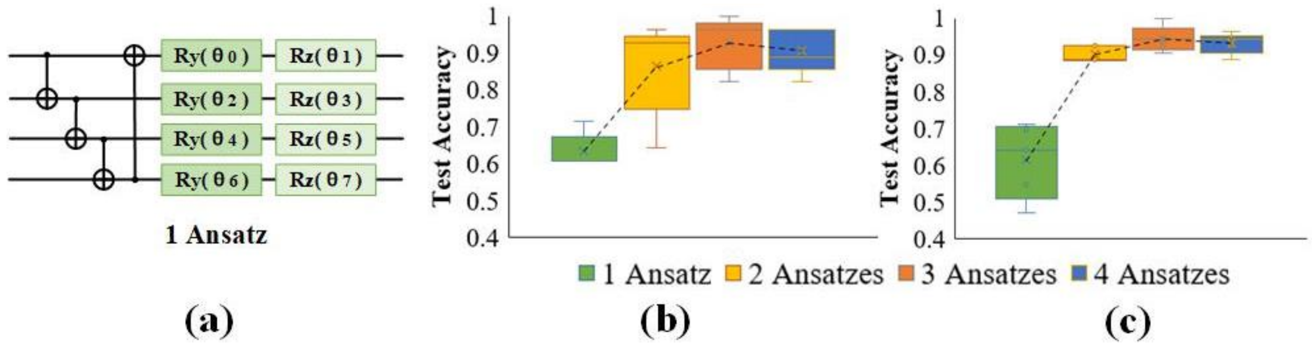

Fig. 6. Test accuracy of HD-EQNN with different numbers of stacked Ansatz layers. Different layers of the Ansatz are stacked to form a QNN. These QNNs constitute the feature extraction module and the ensemble learning classification module, and then form the HD-EQNN. (a) shows the circuit diagram of the 1-layer Ansatz. (b) The test accuracy of Dataset 1. (c) The test accuracy of Dataset 2.

by the number of Ansatz layers in the QNN. The number of Ansatz layers is positively correlated with the model accuracy. As the number of stacked layers increases, the accuracy shows an upward trend. For both Dataset 1 and Dataset 2, the model achieved the highest accuracy when the number of Ansatz layers was 3.

b) Feature extraction module composed of different layers: In this experiment, the influence of feature extraction modules with different layer configurations on the performance of HD-EQNN was investigated. All the QNN structures are the same (with the number of Ansatz layers being 3). Experiment with 4 different structures. In the first experiment, HD-EQNN only retained the ensemble learning classification module. The 128-dimensional features were reduced to 8 dimensions through PCA. In the second experiment, HD-EQNN retained a layer of a feature extraction module and an ensemble learning classification module. During data preprocessing, the 128-dimensional data was reduced to 32 dimensions through PCA. The 32-dimensional reduced-dimensional feature is input into a feature extraction module of one layer, and after extracting 8-dimensional features, it is passed on to an ensemble learning classification module. In the third experiment, the model adopted the complete core structure and reused the previous performance results. In the fourth experiment, on the basis of the complete core architecture, a new feature extraction module was added, and a three-layer feature extraction module was used. The QNN of the ensemble learning classification module was changed from 8-qubit to 2-qubit. After the first two layers of the feature extraction module have extracted the 128-dimensional features into 8-dimensional features, they are then input into the new layer.

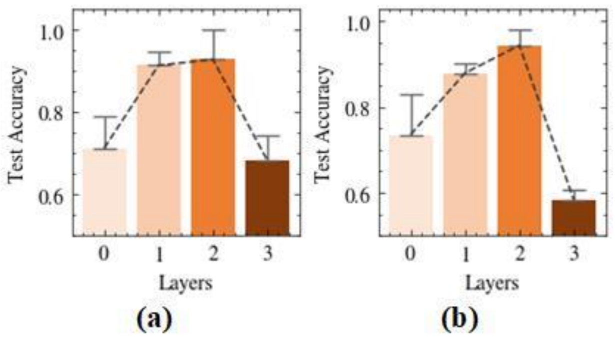

Fig. 7. Test accuracy of different feature extraction modules. (a) The results for Dataset 1. (b) The results for Dataset 2. When using the 2-layer feature extraction module, the accuracy reaches its peak.

The 2-dimensional results extracted from the newly added layer are input into the adjusted ensemble learning classification module, and finally, the classification results are obtained. The experimental results are shown in Fig. 7.

The experimental results demonstrate the impact of different feature extraction modules on the performance of the model. In the first experiment, due to the absence of a feature extraction module, it was impossible to fully extract the valuable information from the 128-dimensional original features, resulting in the poorest performance of the model. The second experiment added a one-layer feature extraction module, which improved the ability of feature extraction, but lost some of the original feature details, and the performance was better than that of the first experiment. In the third experiment, the 128-dimensional original features are gradually compressed and effectively filtered by two layers of feature extraction modules, and then classified by the integrated learning classification module. The feature extraction and classification task had the highest degree of compatibility, thus achieving the optimal performance. The fourth experiment increased the number of layers in the feature extraction module, which also led to an increase in the complexity of the structure. The excessive number of feature extraction modules led to a decrease in the model's efficiency in mapping features, and also introduced additional risks of overfitting, resulting in a significant decline in performance compared to the third experiment. Furthermore, the adjustment of the ensemble learning classification module also affected the accuracy.

The performance of the model in the multi-classification task of identifying radar echo signals from UAVs is influenced by the structure of the feature extraction module. The number of layers in the feature extraction module and the model accuracy have a positive correlation. As the number of layers increases, the accuracy shows an upward trend. For Dataset 1 and Dataset 2, the model achieved the highest accuracy when using the 2-layer feature extraction module.

In summary, on Dataset 1 and Dataset 2, compared to other methods, HD-EQNN achieved the highest multi-classification recognition accuracy. Furthermore, compared to other amplitude-encoded quantum methods, HD-EQNN has a smaller quantum circuit size. The HD-EQNN theoretically possesses stronger anti-decoherence capabilities. HD-EQNN is scalable.

IV. CONCLUSION

Based on the frequency domain characteristics of real UAV radar echo signals, a high-dimensional ensemble quantum neural network was designed to identify various types of UAVs. HD-EQNN is an end-to-end system. The 128-dimensional features are grouped and then rotationally encoded into a model to capture the dependencies. When the pulse repetition period is 1000 μs, the accuracy on the M300, M30T, and CW-10 datasets is 0.9278 ± 0.0719. When the pulse repetition period is 533.3 μs, the accuracy on the Inspire 2, Mavic Air 2, and M300 datasets is 0.9434 ± 0.0353. The performance of HD-EQNN meets the requirements for target recognition and is superior to other quantum methods. Compared with amplitude encoding quantum methods, HD-EQNN has the advantage of a smaller quantum circuit scale and, theoretically, possesses stronger anti-decoherence capability. However, HD-EQNN has certain limitations. On the one hand, the current experimental results are all based on ideal quantum simulators without noise and have not yet been verified on real quantum hardware. On the other hand, HD-EQNN only supports identifying UAVs by analyzing radar echo signals, and it is difficult to effectively integrate and analyze multi-source heterogeneous data, such as text and images.

Next, a noise model will be introduced for robustness testing, and an attempt will be made to deploy HD-EQNN on real quantum hardware. We will also explore quantum machine learning methods that integrate multiple different data modalities for target recognition. This will enhance the understanding ability of HD-EQNN for complex scenarios and give full play to the potential advantages of quantum computing.

ACKNOWLEDGMENT

This work was supported by the National Key R&D Program of China (No. 2024YFB4504100).

REFERENCES

[1] W. Li, Y. Ma, and D.-L. Deng, “Pitfalls and prospects of quantum machine learning,” Nature Computational Science, vol. 5, no. 12, pp. 1095–1097, Dec. 2025.

[2] K. Beer, D. Bondarenko, T. Farrelly, T. J. Osborne, and R. Salzmann, "Training deep quantum neural networks," Nature Communications, vol. 11, no. 1, p. 808, Feb. 2020.

[3] M. Larocca, N. Ju, D. García-Martín, P. J. Coles, and M. Cerezo, "Theory of overparametrization in quantum neural networks," Nature Computational Science, vol. 3, no. 6, pp. 542–551, Jun. 2023.

[4] N. Killoran, T. R. Bromley, J. M. Arrazola, M. Schuld, and N. Quesada, "Continuous-variable quantum neural networks," Physical Review Research, vol. 1, no. 3, Oct. 2019.

[5] A. Abbas, D. Sutter, C. Zoufal, A. Lucchi, and A. Figalli, "The power of quantum neural networks," Nature Computational Science, vol. 1, no. 6, pp. 403–409, Jun. 2021.

[6] M. C. Caro, H.-Y. Huang, M. Cerezo, K. Sharma, and A. Sornborger, "Generalization in quantum machine learning from few training data," Nature Communications, vol. 13, no. 1, Aug. 2022.

[7] Z. Huang, J. Shi, and X. Li, "Quantum few-shot image classification," IEEE Transactions on Cybernetics, vol. 55, no. 1, pp. 194–206, Jan. 2025.

[8] J. Su, X. Zhu, S. Li, and W.-H. Chen, "AI meets UAVs: A survey on AI empowered UAV perception systems for precision agriculture," Neurocomputing, vol. 518, pp. 242–270, Jan. 2023.

[9] M. A. Istiak, M. M. M. Syeed, M. S. Hossain, M. F. Uddin, and M. Hasan, "Adoption of Unmanned Aerial Vehicle (UAV) imagery in agricultural management: A systematic literature review," Ecological Informatics, vol. 78, p. 102305, Dec. 2023.

[10] K. Meng, Q. Wu, J. Xu, W. Chen, and Z. Feng, "UAV-enabled integrated sensing and communication: Opportunities and challenges," IEEE Wireless Communications, vol. 31, no. 2, pp. 97-104, 2023.

[11] H. Jin, X. Jin, Y. Zhou, P. Guo, and J. Ren, "A survey of energy efficient methods for UAV communication," Vehicular Communications, vol. 41, p. 100594, Jun. 2023.

[12] Peyman Aela, H.-L. Chi, A. Fares, T. Zayed, and M. Kim, "UAV-based studies in railway infrastructure monitoring," Automation in Construction, vol. 167, p. 105714, Aug. 2024.

[13] M. Bakirci, "Enhancing vehicle detection in intelligent transportation systems via autonomous UAV platform and YOLOv8 integration," Applied Soft Computing, vol. 164, p. 112015, Oct. 2024.

[14] J. Tian, C. Wang, J. Cao, and X. Wang, "Fully convolutional network-based fast UAV detection in pulse Doppler radar," IEEE Transactions on Geoscience and Remote Sensing, vol. 62, pp. 1-12, 2024.

[15] I. Lam, S. Pant, M. Manning, M. Kubanski, and P. Fox, "Time-frequency analysis using V-band radar for drone detection and classification," in 2023 IEEE International Instrumentation and Measurement Technology Conference (I2MTC), 2023, pp. 1-6.

[16] J. Preskill, "Quantum computing in the NISQ era and beyond," Quantum, vol. 2, p. 79, 2018.

[17] T.-L. Huang, Y.-Z. Wu, M. Ni, S. Wang, and Y.-J. Ye, "Effects of quantum noise on Shor's algorithm," Acta Physica Sinica, vol. 73, no. 5, 2024.

[18] J. Y. Lee, C.-M. Jian, and C. Xu, "Quantum criticality under decoherence or weak measurement," PRX Quantum, vol. 4, no. 3, p. 030317, Aug. 2023.

[19] K. Bharti, A. Cervera-Lierta, T. H. Kyaw, T. Haug, and S. Alperin-Lea, "Noisy intermediate-scale quantum algorithms," Reviews of Modern Physics, vol. 94, no. 1, p. 015004, Feb. 2022.

[20] W. Jiang, J. Xiong, and Y. Shi, "A co-design framework of neural networks and quantum circuits towards quantum advantage," Nature Communications, vol. 12, no. 1, Jan. 2021.

[21] M.-G. Zhou, Z.-P. Liu, H.-L. Yin, C.-L. Li, and T.-K. Xu, "Quantum neural network for quantum neural computing," Research, vol. 6, Jan. 2023.

[22] L. Breiman, "Pasting small votes for classification in large databases and on-line," Machine Learning, vol. 36, no. 1/2, pp. 85–103, 1999.

[23] L. Breiman, "Bagging predictors," Machine Learning, vol. 24, no. 2, pp. 123-140, 1996.

[24] R. J. Doviak and D. S. Zrnic, Doppler Radar & Weather Observations. Academic Press, 2014.

[25] Q. LIN, Z. QIN, L. JIANG, "Ground-based radar detection dataset of 'low slow small' unmanned aerial vehicles under simple field background conditions," Journal of Signal Processing, vol. 40, no. 11, pp. 2095-2104, 2024, doi: 10.12466/xhcl.2024.11.014.

[26] W. Yu and Y. Huang, "Research on classification algorithm for Blackberry Lily data," in Journal of Physics: Conference Series, vol. 1607, no. 1, p. 012099, 2020.

[27] T. K. Ho, "The random subspace method for constructing decision forests," IEEE Transactions on Pattern Analysis and Machine Intelligence, vol. 20, no. 8, pp. 832-844, Aug. 1998.

[28] X. Ding, J. Xu, Z. Song, Y. Hou, and Z. Shan, "Designing quantum multi-category classifier from the perspective of brain processing information," Machine Learning: Science and Technology, vol. 5, no. 3, p. 035070, Sep. 2024.

[29] X. Ding, Z. Song, J. Xu, Y. Hou, and T. Yang, "Scalable parameterized quantum circuits classifier," Scientific Reports, vol. 14, no. 1, p. 15886, Jul. 2024.

[30] W. Wang, J. Xu, F. Liu, B. Zhou, and W. Wang, "Lightweight Quantum Neural Networks Intelligent Generation," Advanced Quantum Technologies, vol. 8, no. 11, Aug. 2025.